ELSEVIER

Journal of Hazardous Materials 141 (2007) 842–849

Journal of Hazardous Materials

www.elsevier.com/locate/jhazmat

# Comparative study on reaction selectivity of azo dye decolorization by *Pseudomonas luteola*

Chung-Chuan Hsueh, Bor-Yann Chen *

*Department of Chemical and Materials Engineering, National I-Lan University, I-Lan 260, Taiwan*

Received 17 May 2006; received in revised form 22 July 2006; accepted 26 July 2006
Available online 31 July 2006

**Abstract**

This study is to inspect how the variation of molecular structures and functional groups present in our model azo dyes (i.e., Congo red, Eriochrome black T (EBT), methyl orange, and methyl red) affects biodecolorization capability of *Pseudomonas luteola*. The most viable decolorization was found at pH 7–9 and the optimal cellular age for the most effective decolorization was 7 days after static incubation in dye-free cultures. In decolorization, the maximal absorption wavelength in UV–vis spectra for the different dye-containing cultures shifted from visible light range towards the ultraviolet visible range. Methyl red was not decolorized in contrast to methyl orange, Congo red, and Eriochrome black T. The sulfonic group *para* to azo bond (–N=N–) in methyl orange was a strong electron-withdrawing group through resonance to cause an enhancement of color removal to be easily biodecolorized. As a charged carboxyl group on methyl red is at *ortho* position (i.e., in the proximity) to azo bond, this led to a complete inhibition to decolorization. However, decolorization of Congo red and EBT in the absence of charged group (e.g., hydroxy or amino group) near azo bond was not completely repressed like methyl red. Thus, the presence of electron-withdrawing groups as the substituents on azo dyes enhanced decolorization capability for biodegradability. In addition, Monod kinetic model provided better predictions to all dye decolorization at initial short periods of time due to negligible intermediate formed at initial short time duration, but significant intermediate accumulation took place at longer period of time. In contrast, the decolorization performances of methyl orange at 400 ppm and EBT at 230 ppm were significantly less than those predicted from the Monod kinetic model likely due to accumulated intermediates exceeding the threshold levels for feedback inhibition.


*Keywords:* Bacterial decolorization; *Pseudomonas luteola*; Azo dye; Chemical structure; Monod kinetics

## 1. Introduction

Azo dyes are the largest chemical class of dyes frequently used for textile dyeing, paper printing, food, and cosmetic. These synthetic dyes that have considerable structural variety are extremely stable under exposure to light and washing, and also resistant to aerobic biodegradation by bacteria [1–3]. The electron-withdrawing characteristics of the azo group and specific substitution patterns generate an electron deficiency, and thus make the compounds recalcitrant to oxidative catabolism [4]. Bacterial degradation of azo dye is often initiated under anaerobic conditions by an enzymatic biotransformation step that involves cleavage of azo linkages [5,6]. The resulting aromatic amines are further degraded by multiple-step bioconversion occurring aerobically or anaerobically [3,7–10].

*Pseudomonas luteola* was predominantly isolated from activated sludge of dyeing wastewater treatment in central Taiwan [11,12]. It was found that the intracellular azoreductase in *P. luteola* is usually an inducible enzyme to specifically deal with azo decolorization. Chang et al. [13] also mentioned certain crucial parameters (e.g., pH, temperature, dissolved oxygen) to affect azo color removal of *P. luteola*. They also suggested that mass transfer resistance of azo dyes across the cell membrane might be the rate-limiting step. In addition, both partial reduction and complete cleavage of the azo bond could contribute to decolorization of monoazo dye reactive red 22 by *P. luteola*. Chen [14] also first provided a toxicological perspective to elucidate decolorization performance of reactive azo dyes. Relatively high toxicity of two azo-bonds present on reactive black B (BB) significantly reduced the decolorization capability of *P. luteola*. In particular, a longer time for persistence of monoazo intermediary metabolites might enhance synergistic toxicity of BB to the bacterial population.

* Corresponding author. Fax: +886 3 9357025.
*E-mail address:* bychen@niu.edu.tw (B.-Y. Chen).

0304-3894/$ – see front matter © 2006 Elsevier B.V. All rights reserved.
doi:10.1016/j.jhazmat.2006.07.056

Considering chemical structure effects, Zimmermann et al. [6] used purified Orange II azoreductase from a *Pseudomonas* strain KF46 to evaluate the decolorization efficiency of various Orange dyes. The specificity of Orange II azoreductase to the surrounding functional groups present in azo dye strongly determined whether the dye is susceptible to biodecolorization. For example, the hydroxy group on the 2-position of the naphthol ring of the azo dye (e.g., 1-(4′-sulfophenylazo)-2-naphthol) is a prerequisite to assist dye decolorization. On the other hand, charged groups near azo bond (e.g., 1-(2′-sulfophenylazo)-2-naphthol) significantly hinder the decolorization efficiency. Moreover, the electron-withdrawing groups present on the phenyl ring accelerate this color removal. Boethling [15], Loonen et al. [16], Suzuki et al. [17] and Jaworska et al. [18] also provided different alternatives to predict biodegradability of organic chemicals from a molecular structure perspective. They all concluded that chemical structures of organic pollutants (e.g., dyes) are of great importance to their biodegradability and also the risk to humans as receptors. As a matter of fact, Boethling [15] tried to evaluate structure/biodegradability relations (so-called SBR); however, it was hampered by a lack of sufficient and consistent data sets. These all are the reasons why we experimentally conducted this study in order to reveal whether chemical structure(s) (e.g., sulfonic acid group) in the proximity of azo bond affect dye decolorization capability of *P. luteola* from various perspectives (e.g., reaction selectivity). The purpose of this study was to compare anaerobic decolorization performance of four water-soluble model dyes (diazo dye—Congo red; naphthol azo dye—Eriochrome black T; monoazo dyes—methyl orange and methyl red) using *P. luteola* and also consider how the difference in dyes affect biodegradability via model predictions of Monod kinetics. In addition, to obtain basic data in common use for comparison, commercial azo dyes (e.g., methyl red and methyl orange) with different functional groups, but not in a related series were used for decolorization testing.

## 2. Materials and methods

### 2.1. Microorganism and culture conditions

*P. luteola* [11] predominantly isolated from activated sludge of a dye-bearing wastewater treatment plant in Taichung, Tai-

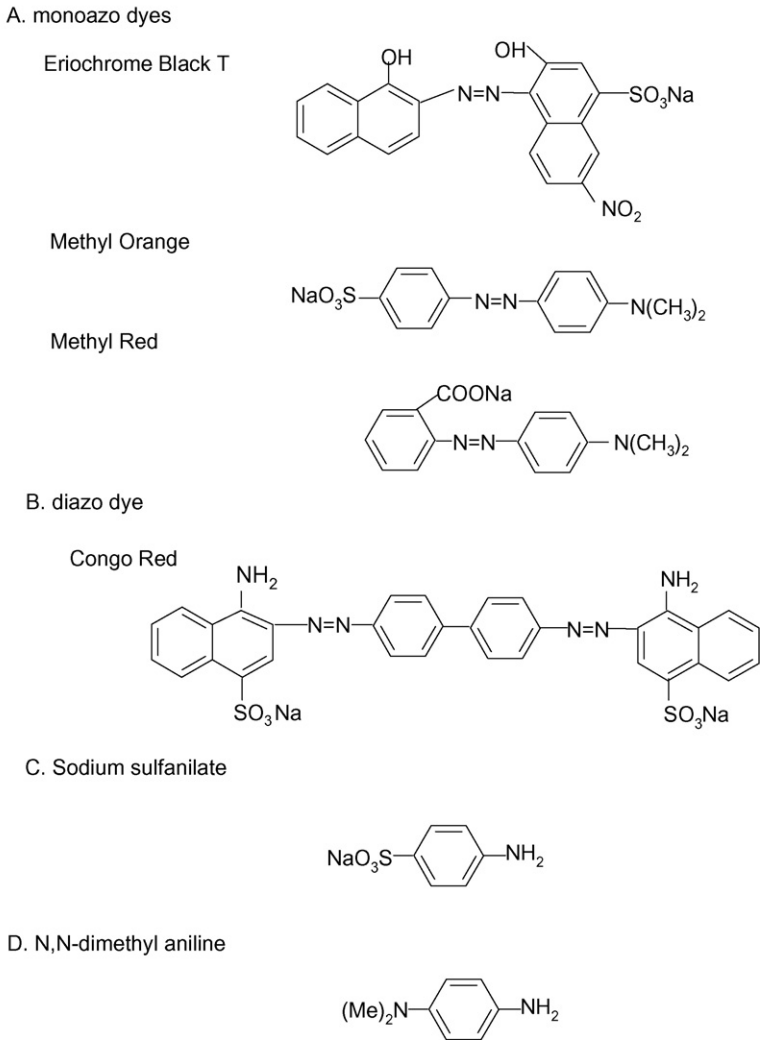


Fig. 1. Chemical structures of azo dyes used in this study, and starting materials of methyl orange—sodium sulfanilate and *N,N*-dimehtyl aniline.

wan, was used as a model strain to indicate decolorization performance [11–13]. To obtain synchrony in the growth phase (i.e., late exponential or early stationary growth phase) of cultures, a loopful of *P. luteola* seed taken from a single colony on a LB-streak plate was precultured in 50-mL Bacto LB broth, Miller (Luria-Bertani (per liter); 10 g Bacto tryptone, 5 g Bacto yeast extract, 10 g sodium chloride) for 24 h at 30 °C, pH 7.0, 125 rpm using a water-bath shaker (SHINKWANG, SKW-12). The 10% (v/v) precultured broth was then inoculated into fresh sterile LB broth for culture. In flask cultures, the pH was not controlled. The initial pH effect was initially adjusted by adding 0.1N $HCl_{(aq)}$ or $NaOH_{(aq)}$. Once cells had been grown to late exponential or early stationary phase (ca. 24 h), shaking was switched off and the culture was kept in static incubation for different periods of time (i.e., 1–13 days) prior to decolorization in order to study the effect of cellular age (i.e., Fig. 2). Decolorization experiments (e.g., Figs. 3 and 4) at various initial dye concentrations were then carried out by using 7-day-old bacteria. Experiments were carried out in duplicate. For comparative decolorization on the same basis, cell concentrations of *P. luteola* were $0.23 \pm 0.03$ g dry cell weight $l^{-1}$.

### 2.2. Chemical and analytical methods

The azo dyes (Fig. 1) used for decolorization were Congo red ($\lambda_{max} = 500$ nm), Eriochrome black T ($\lambda_{max} = 620$ nm) and methyl red ($\lambda_{max} = 540$ nm) (all in JIS special grade) purchased from Wako Pure Chemical Industries Ltd. (Osaka, Japan), and methyl orange ($\lambda_{max} = 465$ nm) obtained from Santoku Chemical Company Ltd. (Osaka, Japan). Dye solutions were sterilized by filtration (Millipore Millex®-GS 0.22 μm filter unit), since these dyes may be unstable in moist-heat sterilization. With appropriate calibrations at specific wavelengths (i.e., $\lambda_{max}$), concentrations of biomass and dyes were determined using an UV–vis spectrophotometer (HITACHI Spectrophotometer, model UV-2001). The dye concentration was determined by measuring the absorbance (Abs) of the cell-free supernatant of the sample at the maximal absorption wavelength (i.e., $\lambda_{max}$) after centrifugation for 2 min at $700 \times g$ (HSIANGTAI Centrifuge MCD-2000). A sterile cell-free medium was chosen as the control. As all samples contained both *P. luteola* and dye to be studied, concentrations of bacterial cells (i.e., (a) and (b)) and dye (i.e., (c)) could be evaluated according to Chen [19,20] as follows:

(a) $Abs_{600\,nm}$ of **the sample mixtures** prior to centrifugation contained measures of cell and dye concentration,
(b) $Abs_{600\,nm}$ of **the sample supernatant** after centrifugation only contained measure of dye concentration at 600 nm and
(c) $Abs_{\lambda_{max}}$ of the sample supernatant after centrifugation was the measure of dye concentration at the maximal absorption wavelength specific to the dye to be tested.

Since the cell concentrations were time-invariant (ca. <10% variation) in different experiments, $Abs_{600\,nm}$ values were not shown and considered as constant. Samples were diluted to an optical density of less than 0.6 when absorbance was not within the linear range (0.1–0.7). The relationship between the cell concentration and $Abs_{600\,nm}$ is 1.0 $Abs_{600\,nm} \cong 0.32$ g dry cell weight $l^{-1}$.

### 2.3. Parameter estimation

To evidently reveal the difference of decolorization capability of *P. luteola* to four azo dyes, time courses of extracellular dye concentration in batch cultures with various initial dye concentrations were used for determination of kinetic parameters. Considering the whole cells of *P. luteola* as enzymes (or biocatalysts), we might apply the Monod kinetic model to depict this decolorization. It is assumed that the cell solution has a fixed number of bioavailable catalysts to which dye substrates can bind. At high substrate concentrations, all these cell catalysts may be occupied by dyes or the biocatalyst is saturated. The scheme of Monod kinetics involves a reversible step for "cell–substrate complex" formation and a dissociation step of the complex. The decolorization rate $V$ can be expressed as follows:

$$V = \frac{-dS}{dt} = \frac{V_m S}{K_S + S}, \quad (1)$$

where $S$, $t$ are dye concentration and elapsed time. Parameters $V_m$ and $K_S$ are the maximal decolorization rate and system coefficient, respectively. Then Eq. (1) can be integrated to obtain:

$$V_m t = (S_0 - S) + K_S \ln\left(\frac{S_0}{S}\right) \quad (2)$$

where $S_0$ is initial concentration of the dye solution.

Kinetic parameters $K_S$ and $V_m$ can then be evaluated from the intercept and slope of the least-squared linear plot $\ln(S_0/S)/(S_0 - S)$ versus $t/(S_0 - S)$ (or similar to Hanes–Woolf plot; Shuler and Kargi [21]). Using these kinetic parameters, time courses of residual dye concentrations were then predicted from Eq. (2) (i.e., predicted curves in Fig. 4b–d).

## 3. Results and discussion

### 3.1. Effects of initial pH and cellular age

To determine the most biologically feasible pH for decolorization, color removal of azo dyes (Congo red, Eriochrome black T, methyl orange, and methyl red; Fig. 1) were conducted

Table 1
Decolorization performance at various initial pHs for different model azo dyes

| | Initial pH | | | | | |
|---|---|---|---|---|---|---|
| | 5 | 6 | 7 | 8 | 9 | 10 |
| Methyl red | − | − | − | − | − | − |
| Methyl orange | − | + | + | + | + | + |
| Eriochrome black T | − | + | + | + | + | − |
| Congo red | − | + | + | + | + | − |

+: Decolorization efficiency $= 1 - \frac{[dye](t=24\,h)}{[dye](t=0)} > 70\%$;
−: decolorization efficiency $= 1 - \frac{[dye](t=24\,h)}{[dye](t=0)} < 10\%$.

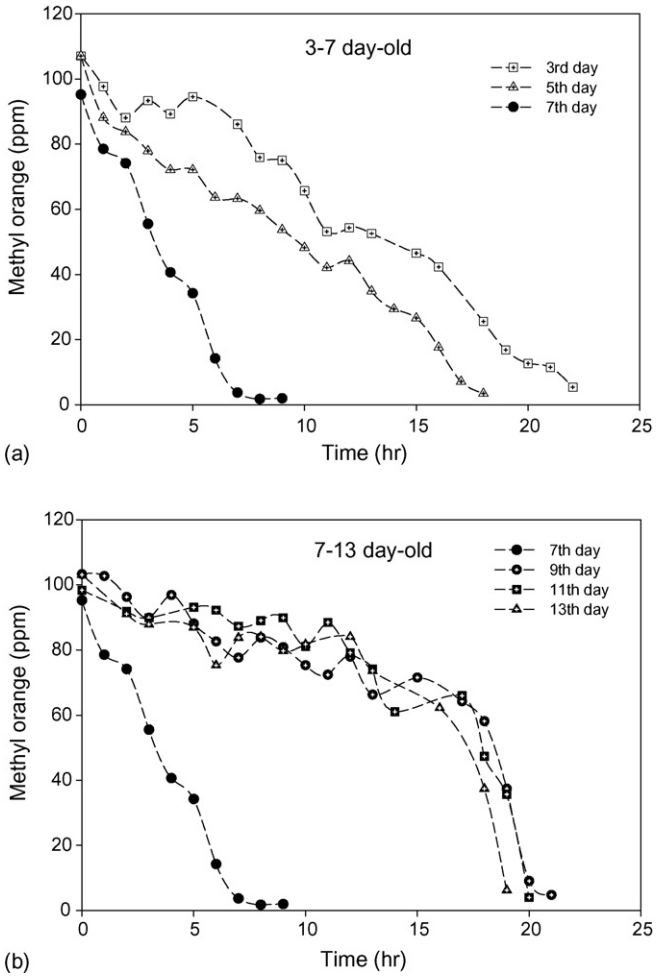


Fig. 2. Time courses of residual concentration of methyl orange using cultures of *P. luteola* in different cellular ages.

at various initial pH levels (i.e., 5–10; Table 1). As clearly indicated in Table 1 all of tested dyes were not appropriate for decolorization at acidic condition (e.g., pH < 5). Methyl red was found to be recalcitrant at any tested pH. In contrast, methyl orange was almost completely decolorized at all pHs other than 5. Congo red and Eriochrome black T could be decolorized at pH 6–9 except at extreme pHs (e.g., 5, 10; Table 1). At pH 10, two hydroxyl groups on EBT near azo bond would be deprotonated to be negatively charged, resulting in impediment of azo dye decolorozation [6]. For methyl orange, this deprotonation near azo bond at pH 10 could not be taken place, thus color removal still occurred at this pH. In low pH azo bonds might include proton to form protonated azo dye (i.e., –N=N– → [–NH–N=]$^+$) and thus *P. luteola* cannot decolorize the azo dye due to this alteration in chemical structures. The most viable decolorization was concluded at ca. pH 7–9. To have a fair comparison for decolorization, dye decolorization was thus carried out at nearly neutral pH.

As the age in various growth phases would also affect the decolorization activity towards azo dyes [11–13,22], different aged-cultures (i.e., 3–13 days old) of *P. luteola* were provided to conduct decolorization of methyl orange (Fig. 2a and b). As indicated in time courses of residual dye concentrations, "younger" aged *P. luteola* (ca. 3–7 days old, Fig. 2a) were more metabolically functioning than older *P. luteola* (ca. 9th to 13th day, Fig. 2b). The optimal age for decolorization was found at 7 days after static incubation in dye-free cultures. It implied that optimal decolorization could be obtained by using medium-older culture. That is, the most feasible cell culture for color removal was at the phase of stationary growth. This suggested that azo dye decolorization is completely non-growth associated [14]. Very likely due to substrate depletion and/or product repression of intermediates, cultures at older ages (ca. 9–13 days; i.e., at relatively late stationary phase) might significantly lose bacterial activity and thus utilize energy for maintenance in cellular survival compared to the optimal age of 7 days. These points all related to decreases in decolorization performance. In addition, longer times for decolorization of older aged-cultures (i.e., >7 days) also suggest that older cells require longer period of time for adaptation in an environment for survival. Moreover, similar cellular age-dependent phenomena were shown in Haug et al. [3]. Even though they used different biodecolorizers (i.e., mixed consortia), their findings are still consistent with our observations for *P. luteola*.

### 3.2. Decolorization characteristics of azo dyes

As shown in UV–vis spectra (Fig. 3a–c), as time went by the maximal wavelength for the different dye-containing cultures shifted from visible light range (i.e., $\lambda_{max}$ for azo dye) towards the ultraviolet visible range (i.e., $\lambda_{max}$ for the aromatic amine intermediate). When the $\pi$ bonds of characteristic conjugated chromophores in an azo dye molecule were broken, the absorption maximal wavelength was shifted towards a shorter wavelength [23]. As the absorption of the shorter-wavelength was represented the higher energy of electronic transition, the azo dye with the characteristic conjugated system of the $\pi$ bonds has the lower energy of electronic transition than aromatic amines (i.e., their intermediates). Similar shifting phenomena could also be observed for decolorization of different dyes (Fig. 3a–c). Fig. 3a clearly pointed out $\lambda_{max}$ of methyl orange is shifted from 465 nm towards 247 nm. As known in organic chemistry, methyl orange can be biodecolorized via the following reaction:

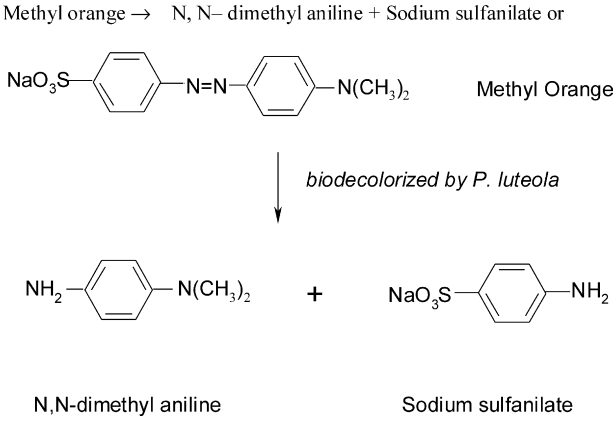


As shown in Fig. 3a, the typical spectrum of sodium sulfanilate was found during decolorization of methyl orange at

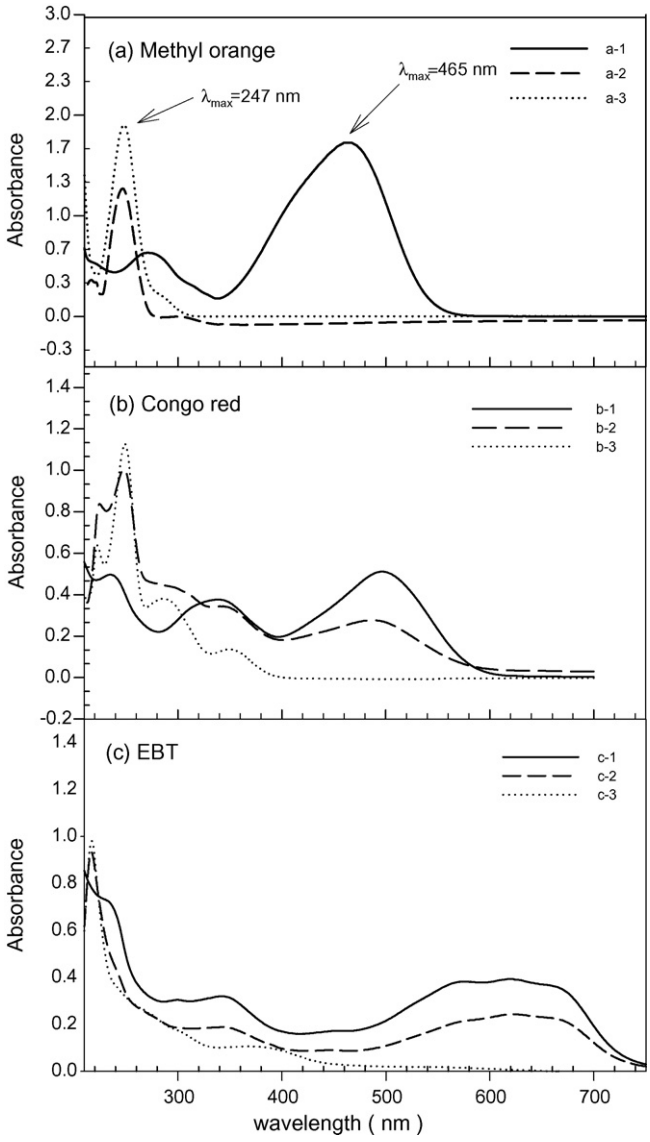


Fig. 3. The UV–vis spectra during decolorization of (a) methyl orange, (b) Congo red and (c) Eriochrome black T at 100 ppm. a-1: intact mehtyl orange; a-2: residual mehtyl orange for 10 h; a-3: sodium sulfanilate. b-1: intact Congo red; b-2: residual Congo red at 3 h; b-3: residual Congo red at 14 h. c-1: intact Eriochrome black T; c-2: residual Eriochrome black T at 2 h; c-3: residual Eriochrome black T at 10 h.

time after 10 h and this point was confirmed afterwards with standard fingerprint of sodium sulfanilate (via the analytical method as described in Hu [11,12]). It directly supported our proposed reaction (shown above) to have sodium sulfanilate as the intermediary product and clearly revealed that no further mineralization was taking place. However, due to low water solubility of *N,N*-dimethyl aniline (NNDA for short) the spectrum of NNDA could not successfully be obtained as anticipated. Fig. 3b and c also indicated that as time went by for decolorization, more significant accumulation of intermediates was resulted due to increased amplitude at the shifted $\lambda_{max}$ (e.g., approx. 500 nm shifted toward 200 nm for Congo red (Fig. 3b) and ca. 620 nm shifted to 220 nm for EBT (Fig. 3c)). Chang et al. [13] suggested that both partial reduction and complete cleavage of the azo bond could contribute to decolorization of reactive red 22 by *P. luteola* via HPLC and GC/MS analyses.

Although methyl orange, EBT and Congo red (Fig. 4b–d) were feasible to be biodecolorized, methyl red was recalcitrant to *P. luteola* at various concentrations (i.e., 100–450 ppm; Fig. 4a). In comparison on these model biodegradable dyes, color removal of methyl orange was the most speedy and efficient (Fig. 4b). For example, its decolorization efficiency of 95% was observed at 6 and 9 h for 100 and 350 ppm, respectively. This result might be explained by the proposed justification in Zimmermann et al. [6] as follows: since the carboxyl group on *ortho*-aminobenzoic acid in methyl red is near azo bond and methyl red (an acid–base indicator ($pK_a = 5.00$) would be in the conjugate base form (i.e., negative-charged form) at neutral pH 7.0, the decolorization is completely inhibited. Zimmermann et al. [6] mentioned that "charged groups in the proximity to the azo group hinder the reaction (i.e., decolorization)." These might clearly explain why methyl red was not biodegradable to *P. luteola*. Compared to other azo dyes, methyl red might be easier to be transported (and/or absorbed) into cellular compartment (e.g., cell plasma) to entice toxicity. Moreover, as the sulfonic group in methyl orange is a stronger electron-withdrawing group than carboxyl group in methyl red and it is *para* to azo bond [24], methyl orange was easily biodecolorized. Although Hu [12] had mentioned "sulfonated substrates for azoreductase exhibited a low $K_m$; however, the reaction velocity decreased. The result was contradictory to Zimmermann et al. [6]." This also indicated that "sulfonated azo dyes were not easily biodegraded" (as Haug et al. [3] stated) should be modified. Here, we verified that sulfonic acid group at appropriate position (e.g., *para* to azo bond) still could enhance azo dye to be biodecolorized by *P. luteola* in this study. In addition, according to Hu [12], sulfonic acid group of three sulfonated azo dyes were all *ortho* to azo bond and thus obstructed decolorization. Our explanations can also be supported by postulates from Knackmuss [4]: xenobiotic compounds (e.g., azo dyes herein) which were reductively degraded under anaerobic condition as the electrophiles (e.g., azo dyes) were the lesser electronic densities, and thus more easily reductively degraded. Zimmermann et al. [6] also revealed that the presence of electron-withdrawing group (e.g., sulfonic group) accelerates anaerobic biodegradation of azo dye. In contrast, for aerobic biodegradation the more electron donating groups present on azo dye are required for a much easier biodegradation as Suzuki et al. [17] stated.

Moreover, although Sugiura et al. [25] mentioned that diazo dye—Congo red was not easily to be biodecolorized, 95% decolorization efficiency of Congo red by *P. luteola* was still observed at 10, 12 h for 110 and 210 ppm, respectively (Fig. 4c). As Congo red is a diazo dye, the maximal decolorization rate of Congo red (Table 2) was less than that of monoazo dye—methyl orange perhaps due to the persistent toxicity of azo bond(s) in Congo red and/or generated intermediates [14,19,20]. In addition, the two-step decolorization was not apparently observed in Fig. 4c perhaps due to lower toxicity and high water solubility to cells. Chen [14] also showed similar toxicity-related decolorization phenomena for different azo dyes (i.e., reactive black B and reactive red 22).

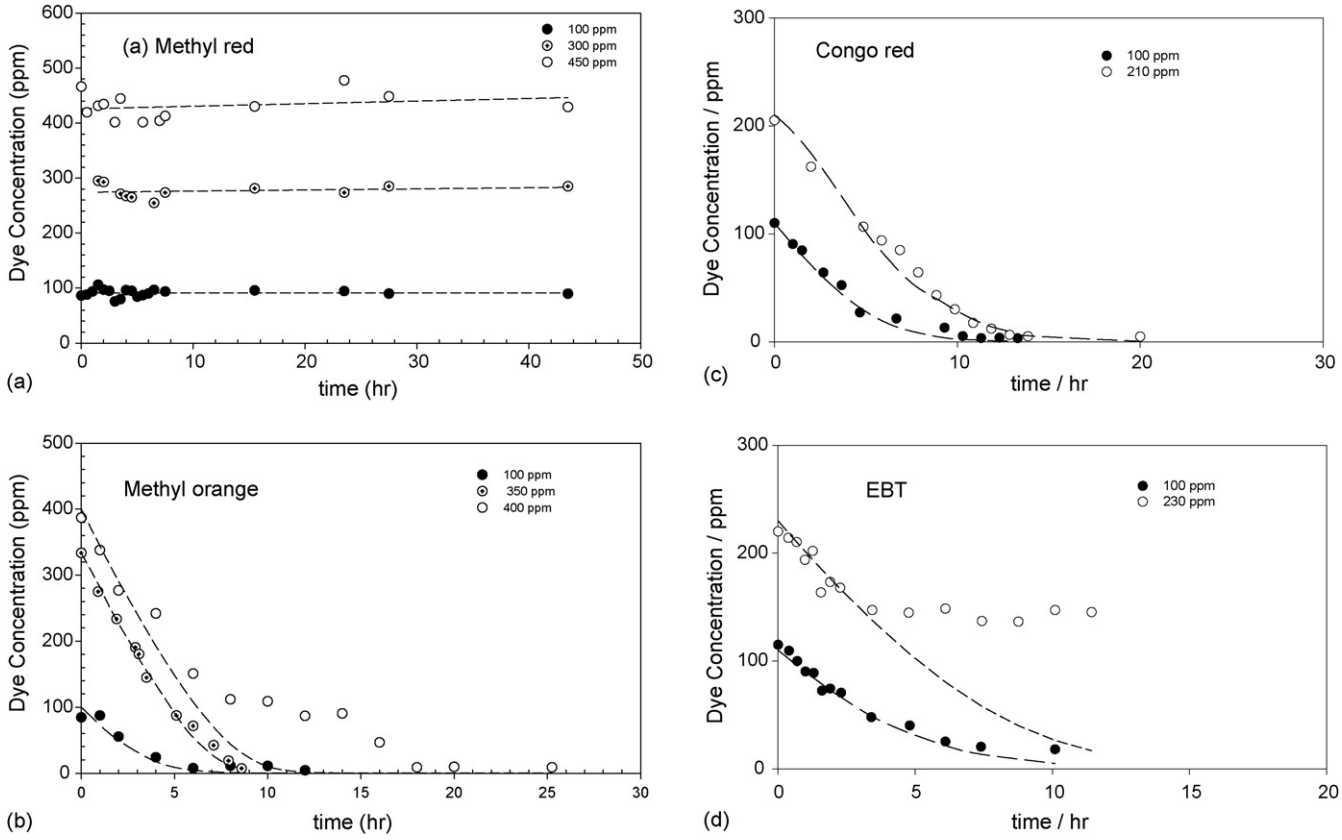


Fig. 4. Time courses of residual concentration of azo dyes (a) methyl red, (b) methyl orange, (c) Congo red, and (d) Eriochrome black T during decolorization of *P. luteola*. The dash curves indicated the results of Monod kinetic model prediction except (a).

In addition, Chung and Stevens [26] indicated that naphthol azo dye—Eriochrome black *T* is also not easily to be biodecolorized, but as shown in Fig. 4d, decolorization of Eriochrome black *T* was almost reached an efficiency of 86% for 110 ppm after 10 h; however, color removal for 230 ppm was completely repressed after ca. 2–3 h (Fig. 4d). The presence of a dinaphthalene group in azo dye may introduce the recalcitrance to dye decolorization. This point is consistent with similar results shown in biodecolorization of amaranth (also a dinaphthalene group containing azo dye; Chung et al. [5] and Haug et al. [3]). Whether dinaphthalene azo dyes were not easily biodegraded or not still remained open to be studied in our further follow-up investigation.

For *P. luteola*, according to previous biodecolorization studies [12–14] and this study, *P. luteola* was highly efficient to decolorization of azo dye, provided that the substituents of azo dyes were not *ortho* to azo bond (i.e., $-CH_3$ in $Y_3GP$ [12] and reactive acid yellow 72 [14], and $-COOH$ in methyl red). That is, sulfonic acid group located at appropriate position (e.g., *para* to azo bond) could still enhance azo dye decolorization by *P. luteola* (e.g., >95% color removal efficiency of methyl orange for 400 mg/l at 20 h). With our novel results, it clearly showed that the biodegradability or recalcitrance is due to combined effects of chemical nature of dyes and biochemical characteristics toward to dyes.

Table 2
Kinetic parameters for decolorization at various azo dyes

| | Methyl orange | Congo red | EBT |
|---|---|---|---|
| Slope | 0.8263 | 0.5423 | 0.4083 |
| Intercept | −0.0188 | −0.0188 | −0.0096 |
| $r^2$ | 0.996 | 0.969 | 0.832 |
| $V_m$ (mg g$^{-1}$ cell min$^{-1}$) | 4.64 | 1.88 | 3.53 |
| $V_m$ (μM g$^{-1}$ cell min$^{-1}$) | 14.2 | 2.70 | 7.66 |
| $K_S$ (ppm) | 53.2 | 53.2 | 104 |
| $K_S$ (μM) | 163 | 76.4 | 226 |

### 3.3. Kinetic analysis

To provide more clues to explain our results, we also carried out kinetic modeling for assessment. Gumport et al. [27] mentioned that "the simple Monod kinetic model applied only to the initial velocity of an enzyme-catalyzed reaction, that is, to the velocity when no appreciable amount of product (e.g., decolorization intermediates) has accumulated." Apparently, this point clearly suggested why Monod kinetic model had better predictions to decolorization of all dyes at some initial period of time due to negligible intermediate (i.e., product P) formed (Fig. 4b–d). On the other hand, as mentioned previously in Section 3.2 (Fig. 4b and d) the decolorization performances of methyl orange at 400 ppm and EBT at 230 ppm were significantly less than those predicted from the Monod kinetic model. The reasons to cause such significant difference are straightforward. Here, we consider a general mechanism

(i.e., $X + S \leftrightarrow XS \leftrightarrow X + P$) that contained four reaction steps (i)–(iv) for cell-catalyzed kinetics as follows:

$$\text{the } k_1 \text{ step}: \quad X + S \xrightarrow{k_1} XS, \tag{i}$$

$$\text{the } k_2 \text{ step}: \quad XS \xrightarrow{k_2} X + S, \tag{ii}$$

$$\text{the } k_3 \text{ step}: \quad XS \xrightarrow{k_3} X + P, \text{ and} \tag{iii}$$

$$\text{the } k_4 \text{ step}: \quad XS \xleftarrow{k_4} X + P \tag{iv}$$

where X, S, XS and P denoted *P. luteola* cells, dye substrate, "cell–substrate complex", and decolorization intermediate, respectively. Note that the product P may denote two or three intermediates instead of one, and be dependent on monoazo or diazo form in the parent dye. As known, the Monod kinetic model can be based upon the assumption of an irreversible $k_3$ step (i.e., $k_4 \cong 0$) and also the XS complex is established rather rapidly. As a matter of fact, the reverse constant, $k_4$, might actually be quite large (e.g., significant intermediate repression) in decolorization compared to $k_3$, but the reverse reaction (iv) still would not occur when little product P (i.e., intermediate) was present since the rate of the $k_4$ step not only depends upon the concentration of X and P but also on the magnitude of $k_4$ [27]. The large differences from Monod kinetic model prediction for methyl orange (400 ppm) and EBT (230 ppm) were likely due to accumulated intermediates (i.e., P) exceeding the threshold levels for inhibition. In addition, the magnitudes of $k_4$ for decolorization of these two dyes might be relatively large and perhaps should not be neglected at higher initial dye concentrations. Considering kinetics parameters, since maximal decolorization rate $V_m$ is $k_3X_0$ and nearly constant cell concentration ($0.23 \pm 0.03$ g dry cell weight $l^{-1}$) were provided a fixed number of active sites of $X_0$ for decolorization, the series of reaction rate constant $k_3$ to break down XS to yield X + P could be obtained as methyl orange (14.2 $\mu M\, g^{-1}$ cell $min^{-1}$) > EBT (7.66 $\mu M\, g^{-1}$ cell $min^{-1}$) > Congo red (2.70 $\mu M\, g^{-1}$ cell $min^{-1}$) (Table 2). As system coefficient $K_S$ is $(k_2 + k_3)/k_1$ (i.e., the ratio of overall dissociation rate constants to association rate constant of XS), a dye with smaller $K_S$ generally tends to have a stronger affinity between enzyme and substrate. The ranking of $K_S$ for azo dyes (or the series of affinity of XS) is EBT > methyl orange > Congo red, very likely indicating a parallel series of binding preference with intracellular azoreductase in *P. luteola* (Table 2).

## 4. Conclusion

The optimal cellular age for the most effective decolorization of the methyl orange was ca. 7 days at pH 7 by *P. luteola*. As a charged carboxyl group on methyl red is at *ortho* position (i.e., in the proximity) to azo bond (–N=N–), this led to a complete inhibition to decolorization in our model azo dyes (i.e., Congo red, Eriochrome black T (EBT), methyl orange, and methyl red) biodecolorized by *P. luteola*. In contrast, as there is no charged group in the proximity to azo bond in Congo red and EBT, decolorization was thus not completely repressed as methyl red. The sulfonic group *para* to azo bond (–N=N–) in methyl orange was a strong electron-withdrawing group by resonance to cause an easy decolorization. Thus, the substituents on azo dyes are the electron-withdrawing groups by resonance to accelerate the decolorizations of azo dyes. Monod kinetic model provided better predictions to all dye decolorization at initial short period of time due to significant intermediate accumulation at longer period of time, but negligible intermediate formed at initial short time duration. In contrast, the decolorization performances of methyl orange at 400 ppm and EBT at 230 ppm were significantly less than those predicted from the Monod model likely due to accumulated intermediates over the threshold levels for inhibition. To obtain conclusive remarks for color removal of *P. luteola*, the follow-up study will investigate serial azo dyes with different functional groups (e.g., electron-releasing groups (e.g., alkyl, amino and hydroxyl groups) and electron-withdrawing groups (e.g., nitro and cyano groups)). As amine intermediates may strongly repress dye decolorization of *P. luteola*, the purification and isolation of these amines via analytical methods (e.g., GC/MS) will be carried out in the follow-up study to identification their possible role in repression. As Connell et al. [28] mentioned that "when exposure (or decolorization) occurs often only a proportion of the chemicals in the bioavailable phase can be taken up by organisms)," the follow-up studies will consider the bioavailability to biodegraders.

## Acknowledgements

Financial supports from National Science Council, Taiwan, R.O.C (NSC 92-2113-M-197-001, NSC 94-2214-E-197-003 and NSC 95-2221-E-197-005) and seeding grants for Biochemical Engineering Laboratory of National I-Lan University (NIU) from the Ministry of Education, Taiwan, R.O.C. were very much appreciated. The authors also extend sincere appreciation to Professor Jo-Shu Chang (Department of Chemical Engineering, National Cheng-Kung University, Tainan, Taiwan) and Professor Tai-Lee Hu (Department of Environmental Engineering and Science, Feng Chia University, Taichung, Taiwan) for kindly suggesting valuable comments and providing strains for the work. The authors also appreciate G.-T. Liu, G.-K. Yu, R.-S. Chen, Y.-M. Huang, Y.-L. Liu, C.-Y. Lu (NIU) for their experimental data analysis. This work is also dedicated to the memory of Dr. Dolloff F. Bishop who passed away on 4 July 1999 when the corresponding author B.-Y. Chen was on duty under his mentorship in National Risk Management Research Laboratory, US Environmental Protection Agency, Cincinnati, Ohio, USA. The authors also appreciate significant comments from the anonymous reviewers.

## References

[1] K. Wuhrman, K. Mechsner, T. Kappeler, Investigation on rate-determining factors in microbial reduction azo dyes, Eur. J. Appl. Microbiol. Biotechnol. 9 (1980) 325–338.

[2] G.M. Shaul, C.R. Dempsey, K.A. Dostal, R.J. Lieberman, Fate of azo dyes the activated sludge process, in: Proceedings Industrial Waste Conference, vol. 41, 1987, pp. 603–611.

[3] W. Haug, A. Schmidt, B. Nortemann, D.C. Hempel, A. Stolz, H.J. Knackmuss, Mineralization of the sulfonated azo dye mordant yellow 3 by 6-aminonaphthalene-2-sulfonate-degrading bacterial consortium, Appl. Environ. Microbiol. 57 (1991) 3144–3149.
[4] H.J. Knackmuss, Basic knowledge and perspectives of bioelimination of xenobiotic compounds, J. Biotechnol. 51 (1996) 287–295.
[5] K.T. Chung, G.E. Fulk, M. Egan, Reduction of azo dyes by intestinal anaerobes, Appl. Environ. Microbiol. 35 (1978) 558–562.
[6] T. Zimmermann, H.G. Kulla, T. Leisinger, Properties of purified orange II azoreductase, the enzyme initiating azo dye degradation by *Pseudomonas* KF46, Eur. J. Biochem. 129 (1982) 197–203.
[7] S. Seshadri, P.L. Bishop, A.M. Agha, Anaerobic/aerobic treatment of selected azo dyes in wastewater, Waste Manage. 14 (1994) 127–137.
[8] E.R. Flores, M. Luijten, B.A. Donlon, G. Lettinga, J.A. Field, Complete biodegradation of the azo dye azodisalicylate under anaerobic conditions, Environ. Sci. Technol. 31 (1997) 2098–2103.
[9] N.C.G. Tan, F.X. Prenafeta-Boldu, J.L. Opsteeg, G. Lettinga, J.A. Field, Biodegradation of azo dyes in cocultures of anaerobic granular sludge with aerobic aromatic amine degrading enrichment cultures, Appl. Microbiol. Biotechnol. 51 (1999) 865–871.
[10] J.A. Libra, M. Borchert, L. Vigelahn, T. Storm, Two stage biological treatment of a diazo reactive textile dye and the fate of the dye metabolites, Chemosphere 56 (2004) 167–180.
[11] T.L. Hu, Decolourization of reactive azo dyes by transformation with *Pseudomonas luteola*, Bioresource Technol. 49 (1994) 47–51.
[12] T.L. Hu, Degradation of azo dye $RP_2B$ by *Pseudomonas luteola*, Water Sci. Technol. 38 (1998) 299–306.
[13] J.S. Chang, C. Chou, Y.C. Lin, P.J. Lin, J.Y. Ho, T.L. Hu, Kinetic characteristics of bacterial azo-dye decolorization by *Pseudomonas luteola*, Water Res. 35 (2001) 2841–2850.
[14] B.Y. Chen, Understanding decolorization characteristics of reactive azo dyes by *Pseudomonas luteola*: toxicity and kinetics, Process Biochem. 38 (2002) 437–446.
[15] R.S. Boethling, Structure/activity relationships for evaluation of biodegradability in the EPA's Office of Pollution Prevention and Toxics, ASTM Special Technical Publication, STP1216 (Environmental Toxicology and Risk Assessment, vol. 2), 1993, pp. 540–544.
[16] H. Loonen, E. Rorije, M. Müller, G. Klopman, W.J.G.M. Peijnenberg, Prediction of biodegradability from chemical structure: modeling of ready biodegradation test data, Environ. Toxicol. Chem. 18 (1999) 1763–1768.
[17] T. Suzuki, S. Timofei, L. Kurunczi, U. Dietze, G. Schuurmann, Correlation of aerobic biodegradability of sulfonated azo dyes with the chemical structure, Chemosphere 45 (2001) 1–9.
[18] J.S. Jaworska, R.S. Boethling, P.H. Howard, Recent developments in broadly applicable structure-biodegradability relationships, Environ. Toxicol. Chem. 22 (2003) 1710–1723.
[19] B.Y. Chen, Toxicity assessment of aromatic amines to *Pseudomonas luteola*: chemostat pulse technique and dose-response analysis, Process Biochem. 41 (2006) 1529–1538.
[20] B.Y. Chen, Revealing threshold criteria of biostimulation for dye-laden wastewater treatment using immobilized cell systems, Process Biochem., in press.
[21] M.L. Shuler, F. Kargi, Bioprocess Engineering: Basic Concepts. Prentice Hall International Series, Prentice-Hall Inc., New Jersey, USA, 1992, pp. 62–67.
[22] B.Y. Chen, J.S. Chang, S.Y. Chen, Bacterial decolourization enhancement using a constructed mixed consortium, J. Chineses Inst. Chem. Eng. 34 (2003) 445–456.
[23] D.A. Skoog, J.J. Leary, Principles of Instrumental Analysis, 4th ed., Saunders College Publishing HBJ, US, 1992, pp. 150–155.
[24] J. McMurry, Organic Chemistry, 6th ed., Brooks/Cole, Belmont, CA, USA, 2004, pp. 539–543.
[25] W. Sugiura, T. Miyashita, T. Yokoyama, M. Arai, Isolation of azo-dye-degrading microorganisms and their application to white discharge printing of fabric, J. Biosci. Bioeng. 88 (5) (1999) 577–581.
[26] K.T. Chung, S.E. Stevens Jr., Degradation of azo dyes by environmental microorganisms and helminths, Environ. Toxicol. Chem. 12 (1993) 2121–2132.
[27] R.I. Gumport, A. Jonas, R. Mintel, C. Rhodes, R.E. Koeppe, Student's Companion to Stryer's Biochemistry, W.H. Freeman and Company, New York, 1990, pp. 95–113 (Chapter 8).
[28] D. Connell, P. Lam, B. Richardson, R. Wu, Distribution and transformation of chemicals in the environment, in: Introduction to Ecotoxicology, Blackwell Science Ltd., Oxford, 1999, pp. 29–49 (Chapter 3).